

# Supporting Information: Towards the Automated Extraction of Structural Information from X-ray Absorption Spectra

Tudur David <sup>1</sup>, Nik Khadijah Nik Aznan <sup>2</sup>, Kathryn Garside<sup>2</sup>, and Thomas J. Penfold <sup>1</sup>

## List of Figures

- S1 Evolution of the MSE as a function of the number of epochs. Data points are obtained from five-times-repeated five-fold cross-validation simulations on the full training set. . . . . 3
- S2 Spectra (*upper*) and  $G^2$  wACSF (*lower*) as a function of spectral shift. Black: Original spectrum, Dark Grey: 1.0 eV shift, Grey: 2.0 eV shift. The six-letter codes are the Cambridge Structural Database identifiers upon which the original spectra are based. . . . . 4
- S3 Spectra (*upper*) and  $G^2$  wACSF (*lower*) as a function of spectral broadening. Black: Original spectrum, Dark Grey: 0.5 eV additional Gaussian Broadening, Grey: 1.0 eV additional Gaussian Broadening and Light Grey: 3.0 eV additional Gaussian Broadening. The six-letter codes are the Cambridge Structural Database identifiers upon which the original spectra are based. . . . . 5
- S4 Example  $G^2$  wACSF predicted from the *held-out* data set using the optimised network. The grey lines are the predicted structures with light grey regions showing  $\pm 2\sigma$  calculated from the bootstrap resampling. The black traces show the true target  $G^2$  wACSF. The upper two panels show predictions from the 0<sup>th</sup>-10<sup>th</sup> percentiles, *i.e.* the best performers when held-out set is ranked by MSE. The centre two panels show predictions from the 45<sup>th</sup>-55<sup>th</sup> percentiles, *i.e.* around the median. The bottom two panels show K-edge XANES spectra from the 90<sup>th</sup>-100<sup>th</sup> percentiles, *i.e.* the lowest performance. The six-character labels in the lower right of each panel are the Cambridge Structural Database (CSD) codes for the samples. . . . . 6
- S5  $G^2$  wACSF predicted from experimental spectra. The source of the experimental spectra is given in Table S1. The grey lines are the predicted structures with light grey regions showing  $\pm 2\sigma$  calculated from the bootstrap resampling. The black traces show the expected  $G^2$  wACSF from experimentally reported structures, as discussed in the main text . . . . . 7
- S6  $G^2$  wACSF predicted from experimental spectra. The source of the experimental spectra is given in Table S1. The grey lines are the predicted structures with light grey regions showing  $\pm 2\sigma$  calculated from the bootstrap resampling. The black traces show the expected  $G^2$  wACSF from experimentally reported structures, as discussed in the main text. . . . . 8

<sup>1</sup>Chemistry - School of Natural and Environmental Sciences, Newcastle University, Newcastle upon Tyne, NE1 7RU, UK, tom.penfold@ncl.ac.uk

<sup>2</sup>Research Software Engineer Group, Catalyst Building, Newcastle University, Newcastle upon Tyne, NE1 7RU, UK

S7	$G^2$ wACSF predicted from experimental spectra. The source of the experimental spectra is given in Table S1. The grey lines are the predicted structures with light grey regions showing $\pm 2\sigma$ calculated from the bootstrap resampling. The black traces show the expected $G^2$ wACSF from experimentally reported structures, as discussed in the main text . . . . .	9
----	---	---

## List of Tables

S1	Name and reference associated with the experimental spectra used in this work. The data is available at [1] . . . . .	10
----	---	----

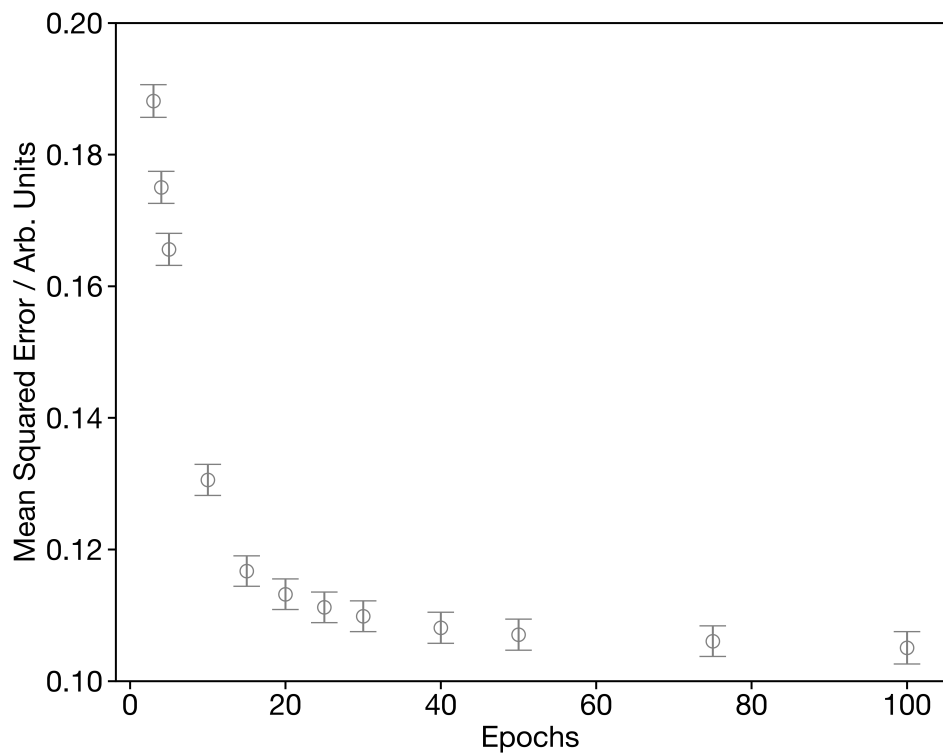


**Figure S1:** Evolution of the MSE as a function of the number of epochs. Data points are obtained from five-times-repeated five-fold cross-validation simulations on the full training set.

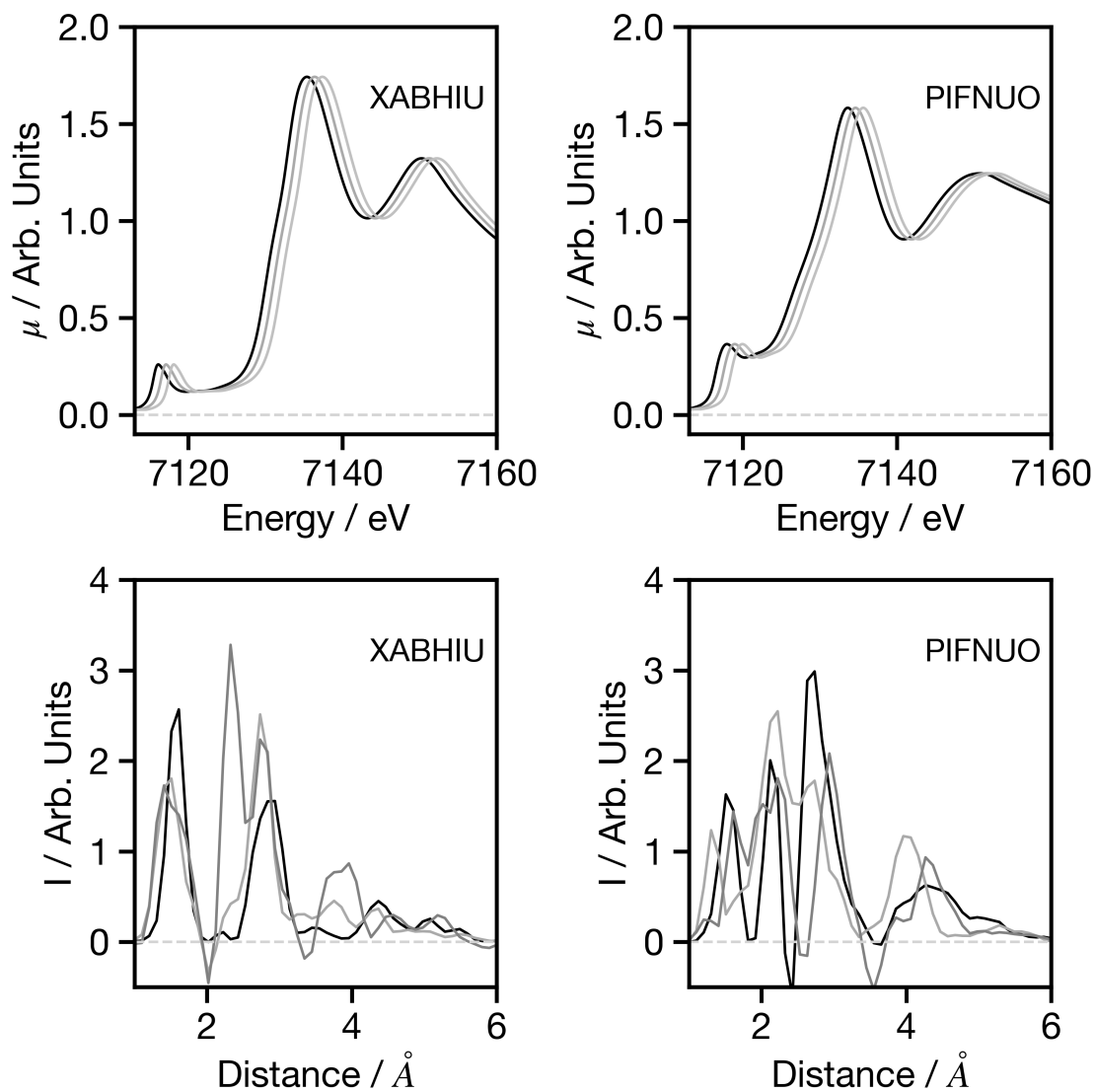


**Figure S2:** Spectra (*upper*) and  $G^2$  wACSF (*lower*) as a function of spectral shift. Black: Original spectrum, Dark Grey: 1.0 eV shift, Grey: 2.0 eV shift. The six-letter codes are the Cambridge Structural Database identifiers upon which the original spectra are based.

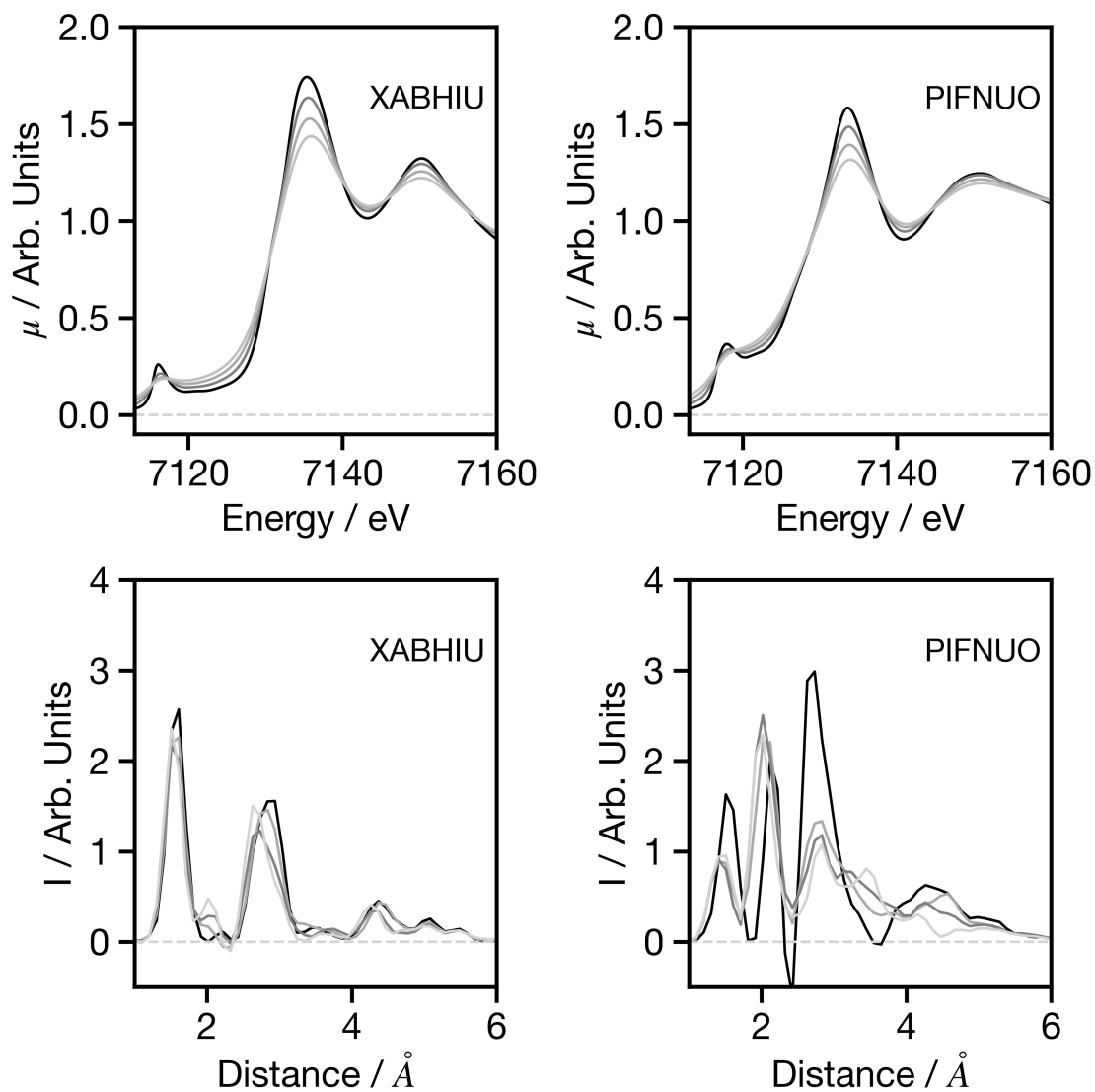


**Figure S3:** Spectra (*upper*) and  $G^2$  wACSF (*lower*) as a function of spectral broadening. Black: Original spectrum, Dark Grey: 0.5 eV additional Gaussian Broadening, Grey: 1.0 eV additional Gaussian Broadening and Light Grey: 3.0 eV additional Gaussian Broadening. The six-letter codes are the Cambridge Structural Database identifiers upon which the original spectra are based.

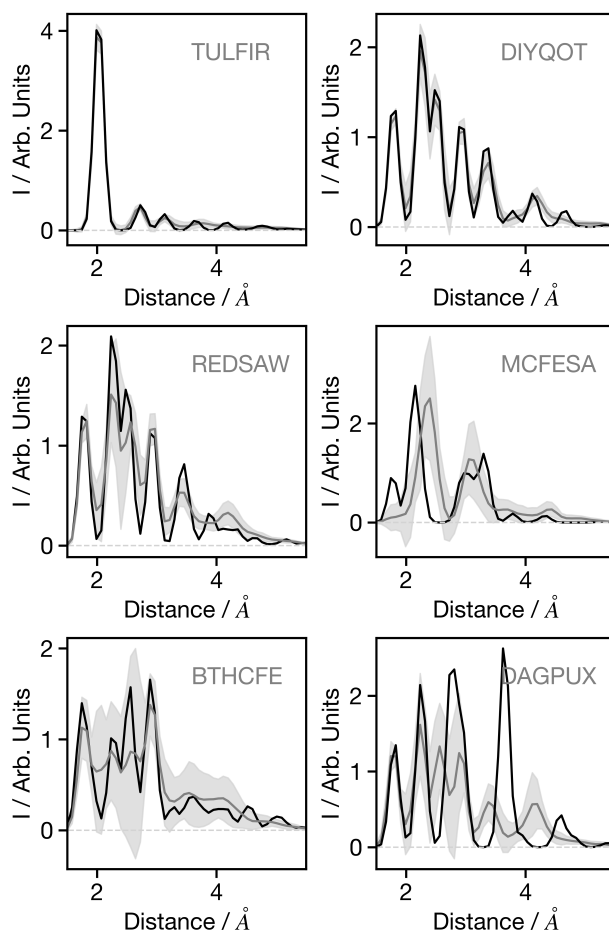


**Figure S4:** Example  $G^2$  wACSF predicted from the *held-out* data set using the optimised network. The grey lines are the predicted structures with light grey regions showing  $\pm 2\sigma$  calculated from the bootstrap resampling. The black traces show the true target  $G^2$  wACSF. The upper two panels show predictions from the  $0^{th}$ - $10^{th}$  percentiles, *i.e.* the best performers when held-out set is ranked by MSE. The centre two panels show predictions from the  $45^{th}$ - $55^{th}$  percentiles, *i.e.* around the median. The bottom two panels show K-edge XANES spectra from the  $90^{th}$ - $100^{th}$  percentiles, *i.e.* the lowest performance. The six-character labels in the lower right of each panel are the Cambridge Structural Database (CSD) codes for the samples.

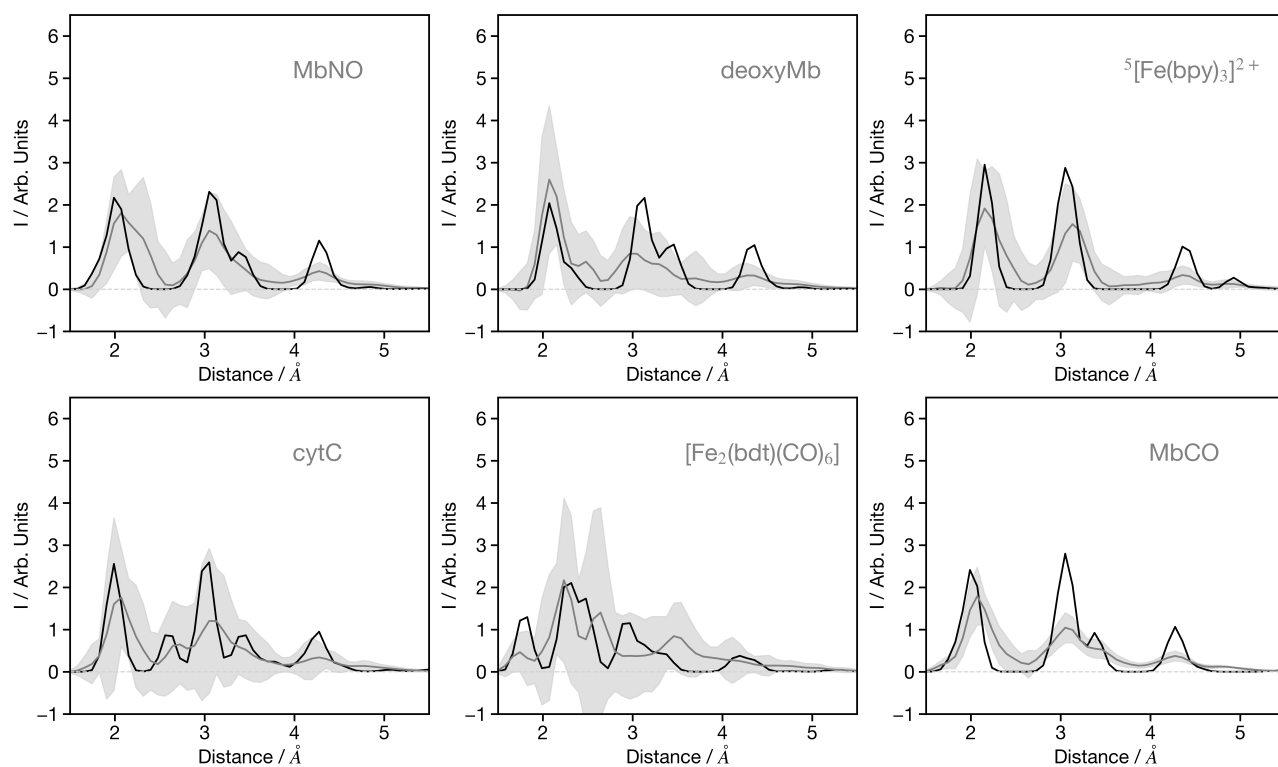


**Figure S5:**  $G^2$  wACSF predicted from experimental spectra. The source of the experimental spectra is given in Table S1. The grey lines are the predicted structures with light grey regions showing  $\pm 2\sigma$  calculated from the bootstrap resampling. The black traces show the expected  $G^2$  wACSF from experimentally reported structures, as discussed in the main text

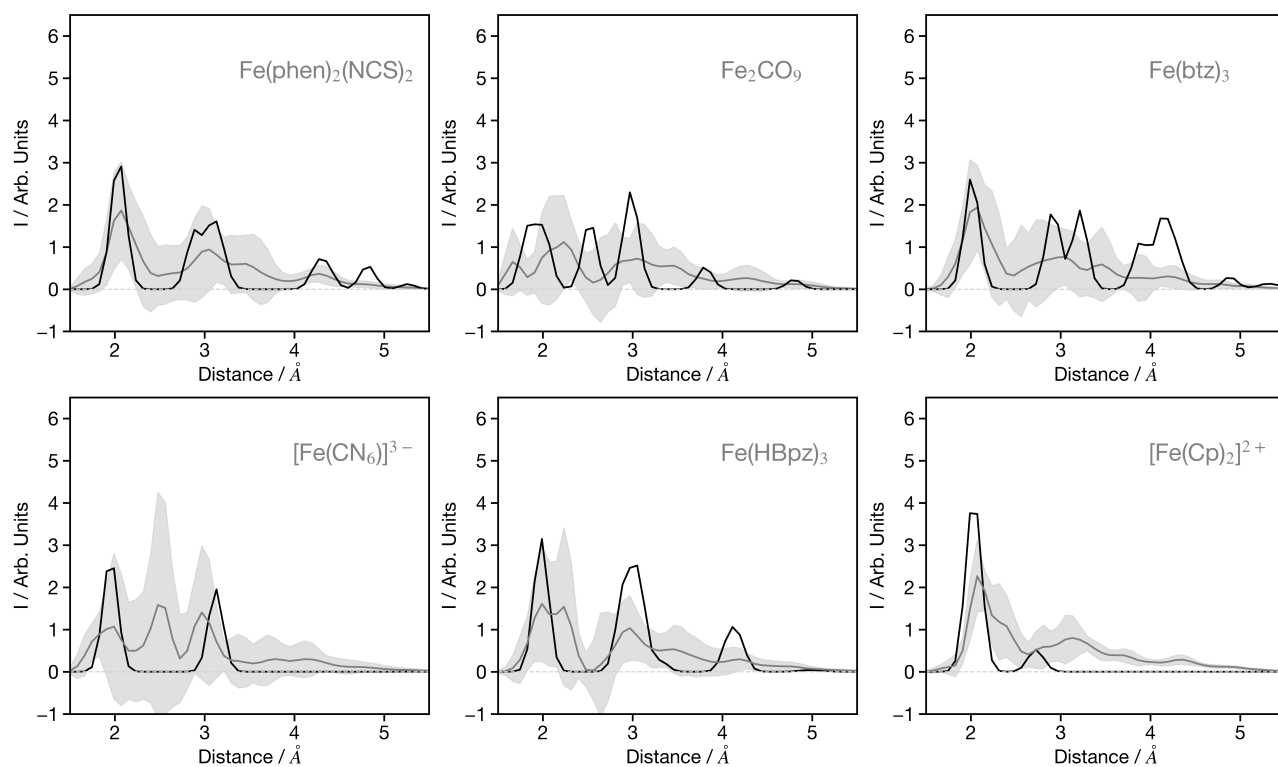


**Figure S6:**  $G^2$  wACSF predicted from experimental spectra. The source of the experimental spectra is given in Table S1. The grey lines are the predicted structures with light grey regions showing  $\pm 2\sigma$  calculated from the bootstrap resampling. The black traces show the expected  $G^2$  wACSF from experimentally reported structures, as discussed in the main text.



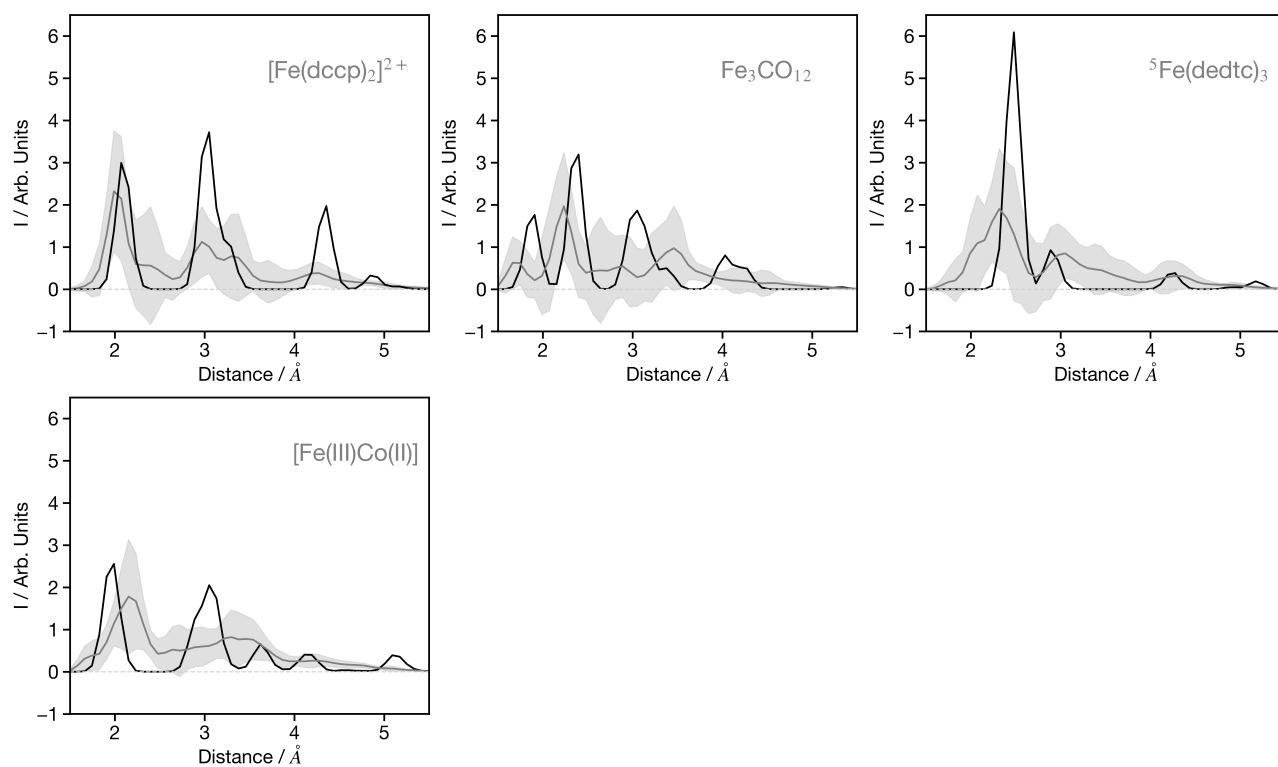


**Figure S7:**  $G^2$  wACSF predicted from experimental spectra. The source of the experimental spectra is given in Table S1. The grey lines are the predicted structures with light grey regions showing  $\pm 2\sigma$  calculated from the bootstrap resampling. The black traces show the expected  $G^2$  wACSF from experimentally reported structures, as discussed in the main text

Compound	Notes	Ref.
<b>MbNO</b>	nitrosylmyoglobin	[2]
<b>MbCO</b>	carboxymyoglobin	[2]
<b>MbO<sub>2</sub></b>	oxymyoglobin	[2]
<b>deoxyMb</b>	unligated myoglobin	[2]
<sup>1</sup> [Fe(bpy) <sub>3</sub> ] <sup>2+</sup>	bpy = 2,2'-Bipyridine	[3]
<sup>5</sup> [Fe(bpy) <sub>3</sub> ] <sup>2+</sup>	bpy = 2,2'-Bipyridine	[3]
<b>cytC</b>	cytochrome C	[4]
<b>Fe(CO)<sub>5</sub></b>		[5]
<b>Fe<sub>2</sub>(CO)<sub>9</sub></b>		[6]
<b>Fe<sub>3</sub>(CO)<sub>12</sub></b>		[6]
<b>Fe<sub>2</sub>(dbt)(CO)<sub>6</sub></b>	dbt = benzenedithiolene	[7]
<b>Fe(phen)<sub>2</sub>(NCS)<sub>2</sub></b>	phen = 1,10-phenanthroline	[8]
<b>Fe(btz)<sub>3</sub></b>	btz = 3,3'-dimethyl-1,1'-bis(p-tolyl)-4,4'-bis(1,2,3-triazol-5-ylidene))	[9]
<b>[Fe(CN)<sub>6</sub>]<sup>4-</sup></b>		[10]
<b>[Fe(CN)<sub>6</sub>]<sup>3-</sup></b>		[10]
<b>Fe(acac)<sub>3</sub></b>		[11]
<b>Fe(HB(pz)<sub>3</sub></b>	pz = pyrazolylborate	[12]
<b>[Fe(Cp)<sub>2</sub>]<sup>2+</sup></b>		[6]
<b>[Fe(dccp)<sub>2</sub>]<sup>2+</sup></b>	dccp = 2,6-(dicarboxypyridyl)pyridine	[13]
<sup>1</sup> [Fe(dedtc) <sub>3</sub> ]	dedtc = N,N'-diethyldithiocarbamate	[8]
<sup>5</sup> [Fe(dedtc) <sub>3</sub> ]	dedtc = N,N'-diethyldithiocarbamate	[8]
<b>[FeIIcOIII]</b>	[(Tp*)Fe(CN)3]2[Co(bpyMe)2]22+	[14]

**Table S1:** Name and reference associated with the experimental spectra used in this work. The data is available at [1]

## References

- [1] XANESNET Training Data, 2023, [gitlab.com/team-xnet/training-sets](https://gitlab.com/team-xnet/training-sets).
- [2] Frederico A Lima, Thomas J Penfold, Renske M Van Der Veen, Marco Reinhard, Rafael Abela, Ivano Tavernelli, Ursula Rothlisberger, Maurizio Benfatto, Christopher J Milne, and Majed Chergui. Probing the electronic and geometric structure of ferric and ferrous myoglobins in physiological solutions by fe k-edge absorption spectroscopy. *Physical Chemistry Chemical Physics*, 16(4):1617–1631, 2014.
- [3] Ch Bressler, C Milne, V-T Pham, Amal EINahhas, Renske M van der Veen, Wojciech Gawelda, S Johnson, Paul Beaud, Daniel Grolimund, Maik Kaiser, et al. Femtosecond xanes study of the light-induced spin crossover dynamics in an iron (ii) complex. *Science*, 323(5913):489–492, 2009.
- [4] Camila Bacellar, Dominik Kinschel, Giulia F Mancini, Rebecca A Ingle, Jérémy Rouxel, Oliviero Cannelli, Claudio Cirelli, Gregor Knopp, Jakub Szlachetko, Frederico A Lima, et al. Spin cascade and doming in ferric hemes: Femtosecond x-ray absorption and x-ray emission studies. *Proceedings of the National Academy of Sciences*, 117(36):21914–21920, 2020.
- [5] Wei-Ting Chen, Che-Wei Hsu, Jyh-Fu Lee, Chih-Wen Pao, and I-Jui Hsu. Theoretical analysis of fe k-edge xanes on iron pentacarbonyl. *ACS omega*, 5(10):4991–5000, 2020.
- [6] Andrew J Atkins, Matthias Bauer, and Christoph R Jacob. High-resolution x-ray absorption spectroscopy of iron carbonyl complexes. *Physical Chemistry Chemical Physics*, 17(21):13937–13948, 2015.
- [7] JPH Oudsen, B Venderbosch, DJ Martin, TJ Korstanje, JNH Reek, and M Tromp. Spectroscopic and theoretical investigation of the [fe 2 (bdt)(co) 6] hydrogenase mimic and some catalyst intermediates. *Physical Chemistry Chemical Physics*, 21(27):14638–14645, 2019.
- [8] Stefan Mebs, Beatrice Braun, Ramona Kositzki, Christian Limberg, and Michael Haumann. Abrupt versus gradual spin-crossover in feii (phen) 2 (ncs) 2 and feiii (dedtc) 3 compared by x-ray absorption and emission spectroscopy and quantum-chemical calculations. *Inorganic Chemistry*, 54(24):11606–11624, 2015.
- [9] Meiyuan Guo, Om Prakash, Hao Fan, Lisa HM de Groot, Valtÿr Freyr Hlynsson, Simon Kaufhold, Olga Gordivska, Nicolás Velásquez, Pavel Chabera, Pieter Glatzel, et al. Herfd-xanes probes of electronic structures of iron ii/iii carbene complexes. *Physical Chemistry Chemical Physics*, 22(16):9067–9073, 2020.
- [10] Thomas James Penfold, Marco Reinhard, Mercedes Hannelore Rittmann-Frank, Ivano Tavernelli, Ursula Rothlisberger, Christopher J Milne, Pieter Glatzel, and Majed Chergui. X-ray spectroscopic study of solvent effects on the ferrous and ferric hexacyanide anions. *The Journal of Physical Chemistry A*, 118(40):9411–9418, 2014.
- [11] Aniruddha Deb and Elton J Cairns. In situ x-ray absorption spectroscopyâa probe of cathode materials for li-ion cells. *Fluid phase equilibria*, 241(1-2):4–19, 2006.

- [12] Valérie Briois, Ph Saintavit, Gary J Long, and Fernande Grandjean. Importance of photoelectron multiple scattering in the iron k-edge x-ray absorption spectra of spin-crossover complexes: full multiple scattering calculations for several iron (ii) trispyrazolylborate and trispyrazolylmethane complexes. *Inorganic Chemistry*, 40(5):912–918, 2001.
- [13] Alexander Britz, Wojciech Gawelda, Tadesse A Assefa, Lindsey L Jamula, Jonathan T Yarranton, Andreas Galler, Dmitry Khakhulin, Michael Diez, Manuel Harder, Gilles Doumy, et al. Using ultrafast x-ray spectroscopy to address questions in ligand-field theory: The excited state spin and structure of [fe (dcpp) 2] 2+. *Inorganic chemistry*, 58(14):9341–9350, 2019.
- [14] Corine Mathonière, Dmitri Mitcov, Evangelia Koumoussi, Daniel Amorin-Rosario, Pierre Dechambenoit, Sadaf Fatima Jafri, Philippe Saintavit, Christophe Cartier dit Moulin, Loic Toupet, Elzbieta Trzop, et al. Metal-to-metal electron transfer in a cyanido-bridged {Fe 2 Co 2} square complex followed by x-ray diffraction and absorption techniques. *Chemical Communications*, 58(86):12098–12101, 2022.